Numerical Investigation of an Unconditionally Stable Compact 2D FDTD Based on the Alternating-Direction Implicit Scheme

Saehoon Ju[1] · Jeongnam Cheon[1] · Hyung-Hoon Kim[2] · Hyeongdong Kim[1]

Abstract

An unconditionally stable compact 2D Alternating-Direction Implicit (ADI) FDTD method for calculating dispersion characteristics of waveguide structures is proposed. The numerical stability and numerical dispersion relation of the proposed method are also presented and discussed. Numerical wavelengths for the dominant and higher order modes in a hollow waveguide are obtained from numerical simulations and compared with those from the analytical dispersion relation. The numerical results show that the proposed scheme has the potential to successfully analyze a class of waveguides having locally fine geometry with reduced numerical costs.

Key words : FDTD, Compact 2D FDTD, ADI Technique, Waveguide.

Ⅰ. Introduction

The compact 2D FDTD method[1]~[5] utilizes the fact that in uniform waveguiding structures the propagating modes take the form $e^{-j\beta z}$ along the propagation direction (z-axis), where β is the propagation constant, and has been used for analyzing dispersion characteristics of waveguiding structures. This method is computationally efficient but its maximum time step size is still bounded by the Courant-Friedrich-Levy (CFL) stability constraint because it is based on the conventional FDTD scheme[2]. This limits the applicability of the method to analyze waveguiding structures of very fine geometry compared with wavelength especially in the field of high-speed circuits and optoelectronics[5],[6].

Recently, to overcome the limit of the stability condition, the alternating direction implicit(ADI) algorithm has been successfully applied to the FDTD method and leads to the unconditionally stable ADI-FDTD method[7]~[9]. It was reported that the ADI-FDTD has the potential to considerably reduce the number of time iterations required to obtain desired responses. Also it was pointed out that the numerical error of the ADI-FDTD algorithm gets worse as the time step $\triangle t$ becomes larger.[8] This numerical error comes dominantly from the numerical dispersion. In a word, the limit of time step Δt for the ADI-FDTD algorithm is not restrained by the stability condition, but by the numerical accuracy.

In this work, we apply the ADI time marching scheme to the conventional compact 2D FDTD method for developing the further efficient analyzing tool for waveguiding structures of fine geometry compared with wavelength. To validate the unconditional stability and the relation between accuracy and time step size, numerical wavelengths for the dominant and higher order modes in a hollow waveguide are obtained from numerical simulations. Numerical wavelengths via the proposed compact 2D ADI-FDTD are compared with our previous work from the analytical dispersion relation[10]. The conventional compact 2D FDTD results [2] and analytical solutions are also presented.

Ⅱ. Formulation of Compact 2D ADI-FDTD

For a waveguide region that is homogeneous and uniform along the propagating z-axis, in the Maxwell equations, the spatial derivatives with respect to z can be expressed as $-j\beta$ because its supporting modes have the propagation constant β along z-axis. Thus, Maxwell equations can be solved over the cross-section of the waveguide and take the following form directly applicable to the so-called compact 2D FDTD method[1],[2].

$$\frac{\partial \vec{H}}{\partial t} = -\frac{1}{\mu}\nabla_{CP2D}\times\vec{E},\quad \frac{\partial \vec{E}}{\partial t} = \frac{1}{\varepsilon}\nabla_{CP2D}\times\vec{H} \tag{1}$$

Manuscript received January 13, 2003 ; revised April 14, 2003.
[1]Department of Electrical and Computer Engineering, Hanyang University, Seoul, 133-791, Korea.
[2]Department of Computer Science, Kwangju Women's University, Kwangju, 506-713, Korea.

, where $\vec{E}$ and $\vec{H}$ are the electric and magnetic fields, ε and μ are the permittivity and permeability, respectively, and ∇_{CP2D} denotes a curl operator whose z derivative term is replaced to $-j\beta$. The conventional compact 2D FDTD[1],[2] can be obtained by directly finite-differencing the eq. (1). However, the proposed compact 2D ADI-FDTD uses the ADI algorithm for time-marching scheme rather than the leapfrog algorithm of the conventional FDTD to circumvent the stability constraint. The ADI algorithm leads that all the field components over the cross-section of the waveguide are evaluated by two sub-iterations:

1st sub-iteration

$$\varepsilon\frac{\partial E_x}{\partial t}\Big|^{n+1/4} = \frac{\partial H_z}{\partial y}\Big|^{n+1/2} + j\beta H_y\Big|^{n}$$

$$\varepsilon\frac{\partial E_y}{\partial t}\Big|^{n+1/4} = -j\beta H_x\Big|^{n+1/2} - \frac{\partial H_z}{\partial x}\Big|^{n}$$

$$\varepsilon\frac{\partial E_z}{\partial t}\Big|^{n+1/4} = \frac{\partial H_y}{\partial x}\Big|^{n+1/2} - \frac{\partial H_x}{\partial y}\Big|^{n}$$

$$\mu\frac{\partial H_x}{\partial t}\Big|^{n+1/4} = -j\beta E_y\Big|^{n+1/2} - \frac{\partial E_z}{\partial y}\Big|^{n}$$

$$\mu\frac{\partial H_y}{\partial t}\Big|^{n+1/4} = \frac{\partial E_z}{\partial x}\Big|^{n+1/2} + j\beta E_x\Big|^{n}$$

$$\mu\frac{\partial H_z}{\partial t}\Big|^{n+1/4} = \frac{\partial E_x}{\partial y}\Big|^{n+1/2} - \frac{\partial E_y}{\partial x}\Big|^{n}$$

2nd sub-iteration

$$\varepsilon\frac{\partial E_x}{\partial t}\Big|^{n+3/4} = \frac{\partial H_z}{\partial y}\Big|^{n+1/2} + j\beta H_y\Big|^{n+1}$$

$$\varepsilon\frac{\partial E_y}{\partial t}\Big|^{n+3/4} = -j\beta H_x\Big|^{n+1/2} - \frac{\partial H_z}{\partial x}\Big|^{n+1}$$

$$\varepsilon\frac{\partial E_z}{\partial t}\Big|^{n+3/4} = \frac{\partial H_y}{\partial x}\Big|^{n+1/2} - \frac{\partial H_x}{\partial y}\Big|^{n+1}$$

$$\mu\frac{\partial H_x}{\partial t}\Big|^{n+3/4} = -j\beta E_y\Big|^{n+1/2} - \frac{\partial E_z}{\partial y}\Big|^{n+1}$$

$$\mu\frac{\partial H_y}{\partial t}\Big|^{n+3/4} = \frac{\partial E_z}{\partial x}\Big|^{n+1/2} + j\beta E_x\Big|^{n+1}$$

$$\mu\frac{\partial H_z}{\partial t}\Big|^{n+3/4} = \frac{\partial E_x}{\partial y}\Big|^{n+1/2} - \frac{\partial E_y}{\partial x}\Big|^{n+1}$$

By applying central difference approximation for the spatial and temporal derivatives to the above equations, we can obtain the system of difference equations for the compact 2D ADI-FDTD. In the same way of the ADI-FDTD[6]~[10], for the sake of updating unknown fields, each of electric field components in sub-iterations can be evaluated by substituting a corresponding magnetic field equation for its unknown magnetic field of the right-hand side and solving a tridiagonal matrix system. The resulting update equations for the 1st sub-iteration step are as follows.

$$\begin{aligned}
&-\frac{(\Delta t)^2}{4\varepsilon\mu(\Delta y)^2}E_x\Big|_{i+1/2,j-1}^{n+1/2} + \left[1+\frac{(\Delta t)^2}{2\varepsilon\mu(\Delta y)^2}\right]E_x\Big|_{i+1/2,j}^{n+1/2} - \frac{(\Delta t)^2}{4\varepsilon\mu(\Delta y)^2}E_x\Big|_{i+1/2,j+1}^{n+1/2} \\
&= E_x\Big|_{i+1/2,j}^{n} + \frac{\Delta t}{2\varepsilon\Delta y}\left(H_z\Big|_{i+1/2,j+1/2}^{n} - H_z\Big|_{i+1/2,j-1/2}^{n}\right) + j\frac{\beta\Delta t}{2\varepsilon}H_y\Big|_{i+1/2,j}^{n} \\
&\quad - \frac{(\Delta t)^2}{4\varepsilon\mu\Delta x\Delta y}\left(E_y\Big|_{i+1,j+1/2}^{n} - E_y\Big|_{i,j+1/2}^{n} - E_y\Big|_{i+1,j-1/2}^{n} + E_y\Big|_{i,j-1/2}^{n}\right)
\end{aligned} \quad (2.a)$$

$$\begin{aligned}
&\left(1+\frac{(\beta\Delta t)^2}{4\varepsilon\mu}\right)E_y\Big|_{i,j+1/2}^{n+1/2} = E_y\Big|_{i,j+1/2}^{n} - \frac{\Delta t}{2\varepsilon}\left(H_z\Big|_{i+1/2,j+1/2}^{n} - H_z\Big|_{i-1/2,j+1/2}^{n}\right) \\
&\quad - j\frac{\beta\Delta t}{2\varepsilon}H_x\Big|_{i,j+1/2}^{n} + j\frac{\beta(\Delta t)^2}{4\varepsilon\mu\Delta y}\left(E_z\Big|_{i,j+1}^{n} - E_z\Big|_{i,j}^{n}\right)
\end{aligned} \quad (2.b)$$

$$\begin{aligned}
&-\frac{(\Delta t)^2}{4\varepsilon\mu(\Delta x)^2}E_z\Big|_{i-1,j}^{n+1/2} + \left[1+\frac{(\Delta t)^2}{2\varepsilon\mu(\Delta x)^2}\right]E_z\Big|_{i,j}^{n+1/2} - \frac{(\Delta t)^2}{4\varepsilon\mu(\Delta x)^2}E_z\Big|_{i+1,j}^{n+1/2} \\
&= E_z\Big|_{i,j}^{n} + \frac{\Delta t}{2\varepsilon\Delta x}\left(H_y\Big|_{i+1/2,j}^{n} - H_y\Big|_{i-1/2,j}^{n}\right) \quad (2.c) \\
&\quad - \frac{\Delta t}{2\varepsilon\Delta y}\left(H_x\Big|_{i,j+1/2}^{n} - H_x\Big|_{i,j-1/2}^{n}\right) + j\frac{\beta(\Delta)^2}{4\varepsilon\mu\Delta x}\left(E_x\Big|_{i+1/2,j}^{n} - E_x\Big|_{i-1/2,j}^{n}\right)
\end{aligned}$$

$$H_x\Big|_{i,j+1/2}^{n+1/2} = H_x\Big|_{i,j+1/2}^{n} - j\frac{\beta\Delta t}{2\mu}E_y\Big|_{i,j+1/2}^{n+1/2} - \frac{\Delta t}{2\mu\Delta y}\left(E_z\Big|_{i,j+1}^{n} - E_z\Big|_{i,j}^{n}\right) \quad (2.d)$$

$$H_y\Big|_{i+1/2,j}^{n+1/2} = H_y\Big|_{i+1/2,j}^{n} + \frac{\Delta t}{2\mu\Delta x}\left(E_z\Big|_{i+1,j}^{n+1/2} - E_z\Big|_{i,j}^{n+1/2}\right) + j\frac{\beta\Delta t}{2\mu}E_x\Big|_{i+1/2,j}^{n} \quad (2.e)$$

$$\begin{aligned}
H_z\Big|_{i+1/2,j+1/2}^{n+1/2} &= H_z\Big|_{i+1/2,j+1/2}^{n} + \frac{\Delta t}{2\mu\Delta y}\left(E_x\Big|_{i+1/2,j+1}^{n+1/2} - E_x\Big|_{i+1/2,j}^{n+1/2}\right) \\
&\quad - \frac{\Delta t}{2u\Delta x}\left(E_y\Big|_{i+1,j+1/2}^{n} - E_y\Big|_{i,j+1/2}^{n}\right)
\end{aligned} \quad (2.f)$$

, where a lossless and homogeneous medium is assumed. The integer i, j indicate that the corresponding basis function is located at $i = i\triangle x$ and $j = j\triangle y$ in the spatial lattice and the index n indicates the temporal grid point, $n = n\Delta t$. In eq. (2), E_x and E_z are updated implicitly and E_y and magnetic fields are calculated explicitly. In the 2nd sub-iteration, electromagnetic fields over the cross-section of a waveguide can be obtained by calculating the following update equations.

$$\left(1+\frac{(\beta\Delta)^2}{4\varepsilon\mu}t\right)E_x\Big|_{i+1/2,j}^{n+1}=E_x\Big|_{i+1/2,j}^{n+1/2}+\frac{\Delta t}{2\varepsilon\Delta y}\left(H_z\Big|_{i+1/2,j+1/2}^{n+1/2}-H_z\Big|_{i+1/2,j-1/2}^{n+1/2}\right)$$
$$+j\frac{\beta\Delta}{2\varepsilon}tH_y\Big|_{i+1/2,j}^{n+1/2}+j\frac{\beta(\Delta t)^2}{4\varepsilon\mu\Delta x}\left(E_z\Big|_{i+1,j}^{n+1/2}-E_z\Big|_{i,j}^{n+1/2}\right)\qquad(3.a)$$

$$-\frac{(\Delta t)^2}{4\varepsilon\mu(\Delta x)^2}E_y\Big|_{i-1,j+1/2}^{n+1}+\left[1+\frac{(\Delta t)^2}{2\varepsilon\mu(\Delta x)^2}\right]E_y\Big|_{i,j+1/2}^{n+1}-\frac{(\Delta t)^2}{4\varepsilon\mu(\Delta x)^2}E_y\Big|_{i+1,j+1/2}^{n+1}$$
$$=E_y\Big|_{i,j+1/2}^{n+1/2}-\frac{\Delta t}{2\varepsilon\Delta x}\left(H_z\Big|_{i+1/2,j+1/2}^{n+1/2}-H_z\Big|_{i-1/2,j+1/2}^{n+1/2}\right)-j\frac{\beta\Delta t}{2\varepsilon}H_x\Big|_{i,j+1/2}^{n+1/2}$$
$$-\frac{(\Delta t)^2}{4\varepsilon\mu\Delta x\Delta y}\left(E_x\Big|_{i+1/2,j+1}^{n+1/2}-E_x\Big|_{i+1/2,j}^{n+1/2}-E_x\Big|_{i-1/2,j+1}^{n+1/2}+E_x\Big|_{i-1/2,j}^{n+1/2}\right)\qquad(3.b)$$

$$-\frac{(\Delta t)^2}{4\varepsilon\mu(\Delta y)^2}E_z\Big|_{i,j-1}^{n+1}+\left[1+\frac{(\Delta t)^2}{2\varepsilon\mu(\Delta y)^2}\right]E_z\Big|_{i,j}^{n+1}-\frac{(\Delta t)^2}{4\varepsilon\mu(\Delta y)^2}E_z\Big|_{i,j+1}^{n+1}$$
$$=E_z\Big|_{i,j}^{n+1/2}-\frac{\Delta t}{2\varepsilon\Delta y}\left(H_x\Big|_{i,j+1/2}^{n+1/2}-H_x\Big|_{i,j-1/2}^{n+1/2}\right)$$
$$+\frac{\Delta t}{2\varepsilon\Delta x}\left(H_y\Big|_{i+1/2,j}^{n+1/2}-H_y\Big|_{i-1/2,j}^{n+1/2}\right)+j\frac{\beta(\Delta t)^2}{4\varepsilon\mu\Delta y}\left(E_y\Big|_{i,j+1/2}^{n+1/2}-E_y\Big|_{i,j-1/2}^{n+1/2}\right)\qquad(3.c)$$

$$H_x\Big|_{i,j+1/2}^{n+1}=H_x\Big|_{i,j+1/2}^{n+1/2}-j\frac{\beta\Delta t}{2\mu}E_y\Big|_{i,j+1/2}^{n+1/2}-\frac{\Delta t}{2\mu\Delta y}\left(E_z\Big|_{i,j+1}^{n+1}-E_z\Big|_{i,j}^{n+1}\right)\qquad(3.d)$$

$$H_y\Big|_{i+1/2,j}^{n+1}=H_y\Big|_{i+1/2,j}^{n+1/2}+\frac{\Delta t}{2\mu\Delta x}\left(E_z\Big|_{i+1,j}^{n+1/2}-E_z\Big|_{i,j}^{n+1/2}\right)+j\frac{\beta\Delta t}{2\mu}E_x\Big|_{i+1/2,j}^{n+1}\qquad(3.e)$$

$$H_z\Big|_{i+1/2,j+1/2}^{n+1}=H_z\Big|_{i+1/2,j+1/2}^{n+1/2}+\frac{\Delta t}{2\mu\Delta y}\left(E_x\Big|_{i+1/2,j+1}^{n+1/2}-E_x\Big|_{i+1/2,j}^{n+1/2}\right)-\frac{\Delta t}{2\mu\Delta x}$$
$$\left(E_y\Big|_{i+1,j+1/2}^{n+1}-E_y\Big|_{i,j+1/2}^{n+1}\right)\qquad(3.f)$$

It should be noted that, unlike the implicit updating of E_x and the explicit updating of E_y in the 1st sub-iteration step, E_x and E_y, respectively, are calculated explicitly and implicitly in the 2nd sub-iteration. This is the result of substituting $-j\beta$ for the spatial derivatives of field components along z-axis. As can be seen in the eq. (2) and eq. (3), the linear system for implicitly updating the electric fields has a tridiagonal matrix form whose elements are coefficients of corresponding three adjacent field components. This linear system can be solved efficiently without matrix inversion via a tridiagonal matrix algorithm.[11] After updating electric field components, magnetic fields components over the cross-section of the waveguide can be calculated fully explicitly from the updated electric fields and previous electromagnetic field components. Therefore we can get the desired solution by selecting a value for β as an input variable and time-marching the proposed algorithm as in the conventional compact 2D FDTD[1],[2].

Ⅲ. Numerical Characteristics of Compact 2D ADI-FDTD

In the compact 2D FDTD[2], the upper limit of stability condition depends on the propagation constant and spatial grid size. However, the proposed compact 2D ADI-FDTD is free from the stability constraint. Theoretically, the unconditional stability can be shown via the Fourier method as described in [7]. From the procedure of the reference [7], a matrix system for time-marching relation can be obtained, i.e. $X^{n+1}=\Lambda X^n$, where the matrix X denotes coefficient matrix of six field components when the field components are expressed as numerical sinusoidal traveling waves at spatially discrete sampled points.

$$\Lambda=\begin{bmatrix}
\frac{A_1+B_3}{\mu^3\varepsilon^3Q_xQ_yQ_z} & \frac{2W_x\cdot W_y}{\mu\varepsilon Q_yQ_z} & \frac{2W_x\cdot W_z}{\mu\varepsilon Q_xQ_z} & \frac{2jW}{\mu\varepsilon^2Q_xQ_z} & \frac{-2jD_2}{\mu^2\varepsilon^3Q_xQ_yQ_z} & \frac{-2jW_y}{\varepsilon Q_yQ_z}\\
\frac{2W_x\cdot W_y}{\mu\varepsilon Q_xQ_y} & \frac{A_2+B_1}{\mu^3\varepsilon^3Q_xQ_yQ_z} & \frac{2W_y\cdot W_z}{\mu\varepsilon Q_xQ_z} & \frac{-2jW_z}{\varepsilon Q_xQ_z} & \frac{2jW}{\mu\varepsilon^2Q_xQ_y} & \frac{-2jD_3}{\mu^2\varepsilon^3Q_xQ_yQ_z}\\
\frac{2W_x\cdot W_z}{\mu\varepsilon Q_xQ_y} & \frac{2W_y\cdot W_z}{\mu\varepsilon Q_yQ_z} & \frac{A_3+B_2}{\mu^3\varepsilon^3Q_xQ_yQ_z} & \frac{-2jD_1}{\mu^2\varepsilon^3Q_xQ_yQ_z} & \frac{-2jW_x}{\varepsilon Q_xQ_y} & \frac{2jW}{\mu\varepsilon^2Q_yQ_z}\\
\frac{2jW}{\mu^2\varepsilon Q_xQ_y} & \frac{-2jW_z}{\mu Q_yQ_z} & \frac{-2jD_1}{\mu^3\varepsilon^2Q_xQ_yQ_z} & \frac{A_1+B_1}{\mu^3\varepsilon^3Q_xQ_yQ_z} & \frac{2W_x\cdot W_y}{\mu\varepsilon Q_xQ_y} & \frac{2W_x\cdot W_z}{\mu\varepsilon Q_yQ_z}\\
\frac{-2jD_2}{\mu^3\varepsilon^2Q_xQ_yQ_z} & \frac{2jW}{\mu^2\varepsilon Q_zQ_y} & \frac{-2jW_x}{\mu Q_xQ_z} & \frac{2W_x\cdot W_y}{\mu\varepsilon Q_xQ_z} & \frac{A_2+B_2}{\mu^3\varepsilon^3Q_xQ_yQ_z} & \frac{2W_y\cdot W_z}{\mu\varepsilon Q_yQ_z}\\
\frac{-2jW_y}{\mu Q_xQ_y} & \frac{-2jD_3}{\mu^3\varepsilon^2Q_xQ_yQ_z} & \frac{2jW}{\mu^2\varepsilon Q_xQ_z} & \frac{2W_x\cdot W_z}{\mu\varepsilon Q_xQ_z} & \frac{2W_y\cdot W_z}{\mu\varepsilon Q_xQ_y} & \frac{A_3+B_3}{\mu^3\varepsilon^3Q_xQ_yQ_z}
\end{bmatrix}$$

$$W=W_xW_yW_z$$
$$A_1=\mu^3\varepsilon^3+\mu^2\varepsilon^2\left(W_x^2-W_y^2-W_z^2\right)+W_x^2W_y^2W_z^2$$
$$A_2=\mu^3\varepsilon^3+\mu^2\varepsilon^2\left(W_y^2-W_z^2-W_x^2\right)+W_x^2W_y^2W_z^2$$
$$A_3=\mu^3\varepsilon^3+\mu^2\varepsilon^2\left(W_z^2-W_x^2-W_y^2\right)+W_x^2W_y^2W_z^2$$
$$B_1=\mu\varepsilon\left(W_x^2W_y^2-W_y^2W_z^2-W_z^2W_x^2\right)$$
$$B_2=\mu\varepsilon\left(W_y^2W_z^2-W_z^2W_x^2-W_x^2W_y^2\right)$$
$$B_3=\mu\varepsilon\left(W_z^2W_x^2-W_x^2W_y^2-W_y^2W_z^2\right)$$
$$D_1=W_y\left(W_x^2W_z^2-\mu^2\varepsilon^2\right)$$
$$D_2=W_z\left(W_y^2W_x^2-\mu^2\varepsilon^2\right)$$
$$D_3=W_x\left(W_z^2W_y^2-\mu^2\varepsilon^2\right)$$

$$W_\alpha=\frac{\Delta t}{\Delta\alpha}\cdot\sin\left(\frac{k_\alpha\Delta\alpha}{2}\right)\quad\alpha=x,y\quad\text{and}\quad W_z=\frac{\beta}{2}$$
$$Q_\alpha=1+\frac{W_\alpha^2}{\mu\varepsilon},\quad\alpha=x,y,z$$

For the compact 2D ADI-FDTD, the eigenvalues of Λ take the following values in eq. (4).

$$\lambda_1=\lambda_4=1,\quad\lambda_2=\lambda_5=(Q+jS)/R,\quad\lambda_3=\lambda_6=(Q-jS)/R\qquad(4.a)$$

$$Q=\mu^3\varepsilon^3-\mu^2\varepsilon^2\left(W_x^2+W_y^2+W_z^2\right)-\mu\varepsilon\left(W_x^2W_y^2+W_y^2W_z^2+W_z^2W_x^2\right)+W_x^2W_y^2W_z^2$$
$$S=2\sqrt{\mu\varepsilon\left(\mu\varepsilon W_x^2+\mu\varepsilon W_y^2+\mu\varepsilon W_z^2+W_x^2W_y^2+W_y^2W_z^2+W_z^2W_x^2\right)\left(\mu^3\varepsilon^3+W_x^2W_y^2W_z^2\right)}$$
$$R=\left(\mu\varepsilon+W_x^2\right)\left(\mu\varepsilon+W_y^2\right)\left(\mu\varepsilon+W_z^2\right)\qquad(4.b)$$

In the compact 2D ADI-FDTD algorithm, W_z is rather than $\Delta t/\Delta z \cdot \sin(k_z \Delta z/2)$ in the conventional 3D ADI-FDTD[6],[7], which relation is obtained by letting $k_z = \beta$ and taking the limit of $\Delta t/\Delta z \cdot \sin(k_z \Delta z/2)$ as $\Delta z \rightarrow 0$[2]. The magnitudes of the eigenvalues are unity because of the relation $Q=\sqrt{R^2-S^2}$ and then the compact 2D ADI-FDTD is unconditionally stable independently from spatial grid size and β. The numerical dispersion relation for the compact 2D ADI-FDTD is derived in a similar manner used in [8] and presented as below:

$$\sin^2\left(\frac{\omega\Delta t}{2}\right)=\frac{\mu\varepsilon\left(W_x^2W_y^2+W_y^2W_z^2+W_z^2W_x^2\right)+\mu^2\varepsilon^2\left(W_x^2+W_y^2+W_z^2\right)}{\left(\mu\varepsilon+W_x^2\right)\left(\mu\varepsilon+W_y^2\right)\left(\mu\varepsilon+W_z^2\right)} \qquad (5)$$

It should be noted out that in eq. (5) the argument of the sine funtion is $\omega\Delta t/2$ rather than in the reference [8] for the sake of comparison with the dispersion relation of the compact 2D FDTD.

In order to demonstrate the unconditional stability and dispersion characteristics of compact 2D ADI-FDTD, the numerical wavelength of a square hollow waveguide is calculated via numerical simulations. The results are compared with compact 2D FDTD results[2], analytic solutions, and numerical wavelengths from the eq. (5):

$$\lambda_{l,m}=\pi c\Delta t\left(\sin^{-1}\left\{\left[\frac{\mu\varepsilon\left(U_x^2U_y^2+U_y^2W_z^2+W_z^2U_x^2\right)+\mu^2\varepsilon^2\left(U_x^2+U_y^2+W_z^2\right)}{\left(\mu\varepsilon+U_x^2\right)\left(\mu\varepsilon+U_y^2\right)\left(\mu\varepsilon+W_z^2\right)}\right]^{\frac{1}{2}}\right\}\right)^{-1} \qquad (6)$$

, where $U_x = \Delta t/\Delta x \cdot \sin(l\pi/2N)$, $U_y = \Delta t/\Delta y \cdot \sin(m\pi/2N)$ and $W_z = \beta\Delta t/2$. The side length of a square air-filled waveguide is a and a/N is used for spatial grid size. To compare with a previous compact 2D FDTD results,[2] the same numerical conditions ($a = 3cm$, $\beta = 209.4395m^{-1}$) are used. Fig. 1. shows relative errors of numerical wavelengths from eq. (6) and eq. (11) in [2] when the Courant number is 0.5. For a value below the Courant limit, compact 2D ADI-FDTD has slightly degraded accuracy compared to compact 2D FDTD. Fig. 2. shows the relative errors of numerical wavelengths from eq. (6) and numerical simulations for $N = 80$ as the Courant number increases. It should be pointed out that simulated results have been obtained by simulating the compact 2D ADI-FDTD with real variables since, in the analysis of hollow waveguide, the eq. (1) can be grouped into two independent and uncoupled subsets[3],[5]. Also, a relatively long window is adapted in the simulation for removing the arificial truncating effect in time doamin. In Fig. 2, we can observe that the numerical wavelength of the compact 2D ADI-FDTD from the analytical dispersion relation of eq. (6) and numerical simulation show an excellent agreement. Note that the compact 2D ADI-FDTD is still stable above the Courant limit but the relative errors are rapidly increasing because the ADI time-stepping algorithm has a second-order accuracy in time, $O(\Delta t^2)$. As can be seen, although the compact 2D ADI-FDTD is unconditionally stable independently from spatial grid size and β, the compact 2D ADI-FDTD should be applied to the problem of analyzing a class of waveguides having locally very fine geometry compared with wavelength to guarantee both computational efficiency and numerical accuracy.

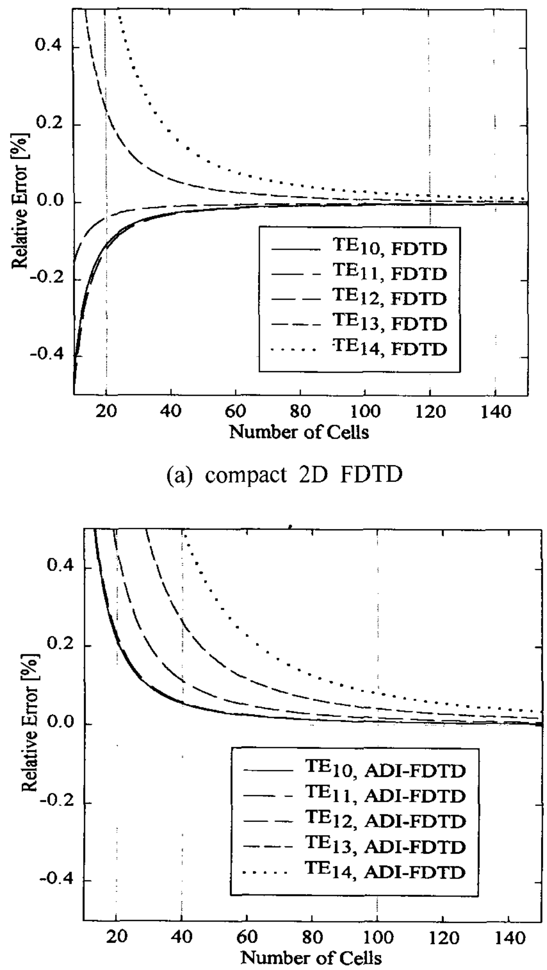

(a) compact 2D FDTD

(b) compact 2D ADI-FDTD

Fig. 1. The relative error of the numerical wavelength versus the number of cells, N. The side length of a waveguide, a, is $3cm$, β is $209.4395m^{-1}$, and the Courant number is 0.5.

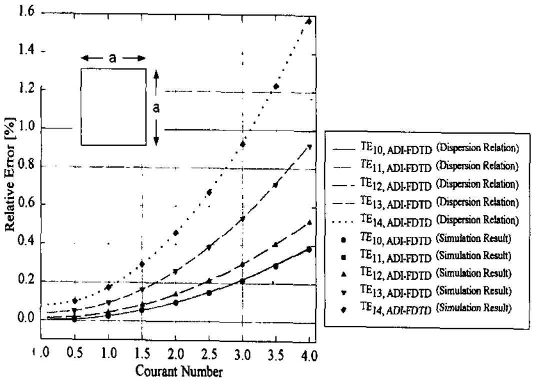

Fig. 2. The relative error of the numerical wavelength versus the Courant number. The side length of a waveguide, *a*, is $3cm$, β is $209.4395m^{-1}$, and the number of cells, *N*, is 80. In the simulation, the time step is chosen as 20000 $\triangle t_{CFL=1}$, where $\triangle t_{CFL=1}$, denotes the limit of CFL stability condition.

Ⅳ. Conclusion

We have proposed an unconditionally stable compact 2D FDTD scheme for the analysis of waveguiding structures using the ADI time-marching scheme. The numerical wavelengths of the dominant and higher order modes in a hollow waveguide are simulated by the proposed method and compared with the conventional compact 2D FDTD results, analytical solutions, and the wavelengths from analytical dispersion relation. Numerical results show that the proposed compact 2D ADI-FDTD scheme could be used to efficiently analyze various waveguides of locally fine geometries.

References

[1] A. Asi, L. Shafai, "Dispersion analysis of aniotrcpic inhomogeneous waveguides using compact 2D-FDTD", *Electron. Lett.*, vol. 28, pp. 1451-1452, Jul. 1992.

[2] A. C. Cangellaris, "Numerical stability and numerical dispersion of a compact 2-D/FDTD method used for the dispersion ananlysis of waveguides", *IEEE Microwave Guided Wave Lett.*, vol. 3, pp. 3-5, Jan. 1993.

[3] S. Xiao, R. Vahldieck, "An efficient 2-D FDTD algorithm using real variables", *IEEE Microwave Guided Wave Lett.*, vol. 3, pp. 127-129, May 1993.

[4] A. P. Zhao, J. Juntunen and A. V. Räisänen, "Relationship between the compact complex and real variable 2-D FDTD methods in arbitrary anisotropic dielectric waveguides", in *IEEE MTT-S Int. Microwave Symp. Dig.*, vol. 1, pp. 83-87, 1997.

[5] F. Zepparelli, P. Mezzanotte, F. Alimenti, L. Roselli, R. Sorrentino, G. Tartarini and P. Bassi, "Rigorous analysis of 3D optical and opto-electronic devices by the compact-2D-FDTD method", *Optical and Quantum Electronics*, vol. 31, pp. 827-841, Oct. 1999.

[6] A. Taflove, S. C. Hagness, *Computational Electrodynamics: The Finite-Difference Time-Domain Method,* 2nd ed., Norwood, MA: Artech House, 2000.

[7] F. Zheng, Z. Chen and J. Zhang, "Toward the development of a three-dimensional unconditionally stable finite-difference time-domain method", *IEEE Trans. Microwave Theory and Tech.*, vol. 48, pp. 1550-1558, Sep. 2000.

[8] F. Zheng, Z. Chen, "Numerical dispersion analysis of the unconditionally stable 3-D ADI- FDTD method", *IEEE Trans. Microwave Theory and Tech.*, vol. 49, pp. 1006-1009, May 2001.

[9] T. Namiki, "3-D ADI-FDTD methodunconditionally stable time-domain algorithm for solving full vector Maxwell"s equations", *IEEE Trans. Microwave Theory and Tech.*, vol. 48, pp. 1743-1748, Oct. 2000.

[10] S. Ju, H. Kim, "Investigation of an unconditionally stable compact 2D ADI-FDTD algorithm: formulations, numerical stability, and numerical dispersion", in *IEEE AP-S Int. Symp. Dig.*, vol. 3, pp. 639-642, 2002.

[11] W. H. Press, B. P. Flannery, S. A. Teukolsky and W. T. Vetterling, *Numerical Recipes in C,* New York, NY: Cambridge Press, 1988.

Saehoon Ju

was born in Seoul, Korea, in 1974. He received the B.S. and M.S. degrees in 1997 and 1999, respectively, from Hanyang University, Seoul, Korea. From Apr. 1999 to Mar. 2000, he was a Research Assistant at UARC (Underwater Acoustics Research Center) in Seoul National University, Seoul, Korea, and is currently working toward the Ph.D. degree in Hanyang University, Seoul, Korea. In Sept. 2002, he rejoined the UARC in Seoul National University, Seoul, Korea, as a research Assistant. His research interests are the computational methods for electromagnetic problems, the wavelet domain methodology of various electromagnetic problems such as scattering, waveguide discontinuities, signal integrity analysis, and the ultra-wideband short-pulse electromagnetics.

Jeongnam Cheon

was born in Jeollabuk-do, Korea, in 1975. He received the B.S. and M.S. degrees in 1998 and 2000, respectively, from Hanyang University, Seoul, Korea, both in electrical and computer engineering. He is currently pursuing the Ph.D. degree at the same university. His research interests are the time domain computational methods using the wavelet transform and alternating direction implicit concepts, respectively, the electromagnetic modeling for signal integrity analysis of high-speed electronic circuits, and the electromagnetic compatibility assessment of integrated electronic circuits.

Hyung-Hoon Kim

was born in Kwang-ju, Korea. He received the B.S. degree form Chonnam National University, Kwang-ju, Korea, in 1986 and the M.S. degree form Korea Institute of Science and Technology, Seoul, Korea, in 1988. From Mar. 1988 to Sep. 1990, he was a Researcher at R&D center in KIA Motors Corp. From Sep. 1990 to Jul. 1994, he was a Senior Researcher at HumanCom Inc. In Sep. 1994, he joined the Department of Computer Science, Kwang-ju Women"s University, Kwang-ju, Korea, as a Professor. Also, from Mar. 1995, he has been working toward the Ph.D. degree in Chonnam National University, Kwang-ju, Korea. His main research interest is the development of computer algorithms for information security.

Hyeongdong Kim

was born in Kwang-ju, Korea. He received the was born in Kwang-ju, Korea. He received the B.S. and M.S. degrees from Seoul National University, Seoul, Korea, in 1984 and 1986, respectively, and the Ph.D. degree from the University of Texas at Austin in 1992. From May 1992 to Feb. 1993, he was a Post-Doctoral Fellow in the University of Texas at Austin. From 1993 to 1999, he was an Assistant Professor in the Department of Electrical and Computer Engineering, Hanyang University, Seoul, Korea, and now he is an Associate Professor at the same university. His research interests are the computational electromagnetics using the wavelet transform concept, the application area of which is the microwave engineering, the electromagnetic modeling for signal integrity analysis of high-speed electronic circuits, the development of microwave circuits for software-defined radio systems, and the electromagnetic compatibility assessment of packaged integrated electronics.